

## Scaling law of the giant Stark effect in boron nitride nanoribbons and nanotubes

Fawei Zheng,<sup>1</sup> Zhirong Liu,<sup>2</sup> Jian Wu,<sup>1</sup> Wenhui Duan,<sup>1,\*</sup> and Bing-Lin Gu<sup>1</sup><sup>1</sup>Department of Physics, Tsinghua University, Beijing 100084, People's Republic of China<sup>2</sup>College of Chemistry and Molecular Engineering, Peking University, Beijing 100871, People's Republic of China

(Received 29 June 2008; published 19 August 2008)

*Ab initio* calculations reveal a universal scaling law on how the electronic structure of boron nitride (BN) nanoribbons and nanotubes is modified by a transverse electric field. Due to the structural symmetry difference, the energy gap of zigzag BN ribbons can be reduced or increased by the electric field depending on the sign of the field, while that of the armchair ones is always reduced. However, the linear giant Stark effect coefficients of zigzag and armchair BN nanoribbons, as well as those of BN nanotubes, are found to obey a unified scaling law where the coefficient increases linearly with the ribbon width or the tube diameter with a slope of 1.0. The mechanism of the scaling law is identified using a general model, which may be applicable to other semiconducting nanostructures.

DOI: 10.1103/PhysRevB.78.085423

PACS number(s): 73.22.-f, 71.70.Ej, 71.20.Nr

A key factor underlying nanoscience and nanotechnology is the ability to tune the novel properties of nanostructures in a controlled way. To modify the electric properties of nanostructures, gate voltages or electric fields are usually utilized in nanoelectronic devices. For one-dimensional nanostructures, when a transverse electric field is applied, the energy gap will be changed and gap opening and closure may be induced under high fields. This effect, named the giant Stark effect, has been theoretically studied on carbon nanotubes (CNTs),<sup>1–6</sup> boron nitride nanotubes (BNNTs),<sup>3,7</sup> and BN nanoribbons (BNNRs) (Refs. 8–10) and has been experimentally observed by optical spectra<sup>11</sup> and scanning tunneling microscopy<sup>12</sup> measurements. The electric field may also couple with magnetic properties of nanostructures.<sup>9,13</sup> Recently, Son *et al.*<sup>13</sup> showed that the high in-plane transverse electric field would induce half metallicity in zigzag graphene nanoribbons (GNRs), which may have many potential applications in spintronics. Moreover, the graphene nanoribbons were predicted to exhibit diverse transport behavior under bias voltage (electric field) or gate voltages such as doping-induced spin-anisotropic scattering,<sup>14</sup> switching as valley filter and valley valve,<sup>15</sup> and unique mirror-symmetry dependency.<sup>16</sup>

The performance of nanostructures usually depends on the size of the systems in a delicate way. Some elegant scaling laws have been revealed. Perhaps the most famous is the dependence of the electronic structure of CNTs on their chirality and diameter:<sup>17</sup> all armchair CNTs are metallic, while  $(n, 0)$  zigzag CNTs are metallic if  $n/3$  is an integer and semiconducting otherwise. When the finite length is considered, the energy gap  $E_g$  of armchair CNTs decreases with the tube length in a well-defined oscillation with the period of  $3a/2$ , where  $a$  is the lattice constant,<sup>18</sup> together with a long periodic oscillation.<sup>19</sup> In armchair GNRs, the semiconducting characteristic is mainly determined by quantum confinement and can be approximately described<sup>20</sup> by  $E_g \sim 1/w$  where  $w$  is the width or by more accurate analytic scaling rules including the effect of the edges.<sup>21</sup> For the giant Stark effect, great efforts<sup>1–12</sup> have been made to investigate how the electronic structures are modulated by the electric field and many characteristics have been elucidated, e.g., the gap modulation increases with tube diameter and the effect is more dramatic

in BNNTs than in CNTs due to a reduced screening of the electric field. However, a systematic comparative study on the giant Stark effect of various nanostructures to reveal a possible general scaling law is still lacking.

In this work, using *ab initio* calculations and model analysis, we investigate the giant Stark effect in BN nanoribbons and nanotubes under a transverse electric field and explore the common scaling behaviors in these nanostructures. It is shown that the symmetry of systems has fundamental influence on the effect of electric fields. For symmetric cases such as nanotubes and armchair BNNRs (ABNNRs), the electric field will mix the nearby states in the valence band and those in the conduction band separately, which always leads to a reduction in the energy gap. For asymmetric cases such as zigzag BNNRs (ZBNNRs), however, a transverse polarization spontaneously exists so that the state mixing is not necessary for the Stark effect and the electric field could either decrease or increase the energy gap depending on its direction. Interestingly, no matter whether the systems are symmetric or asymmetric, their linear Stark effect coefficients all increase with the width, scaling into a universal straight line with a predicted slope of 1.0.

The systems investigated here include BNNTs and BNNRs. The emphasis was put on BNNRs because BNNRs may be symmetric or asymmetric while responding to the electric field, and also because the fully passivated BNNRs are wide gap semiconductors independent of their widths and chiralities and thus it would be desirable to tune their energy gap. In experiments, single-layer *h*-BN has been successfully fabricated on the surfaces of metals.<sup>22–24</sup> BNNRs are expected to be produced by cutting single-layer *h*-BN but may have very different properties due to the quantum confinement effect and the appearance of the edge states originated from their specific structures. When the edges are partially passivated, zigzag BNNRs may exhibit half metallicity,<sup>25</sup> which makes them good candidates for spintronic applications.

Our calculations were performed using the density-functional theory method, within the local-density approximation for exchange-correlation, and norm-conserving pseudopotentials.<sup>26</sup> We carried out the calculations employing the SIESTA code.<sup>27</sup> Integration over the one-dimensional Brillouin zone has been carried out by using the Monkhorst-

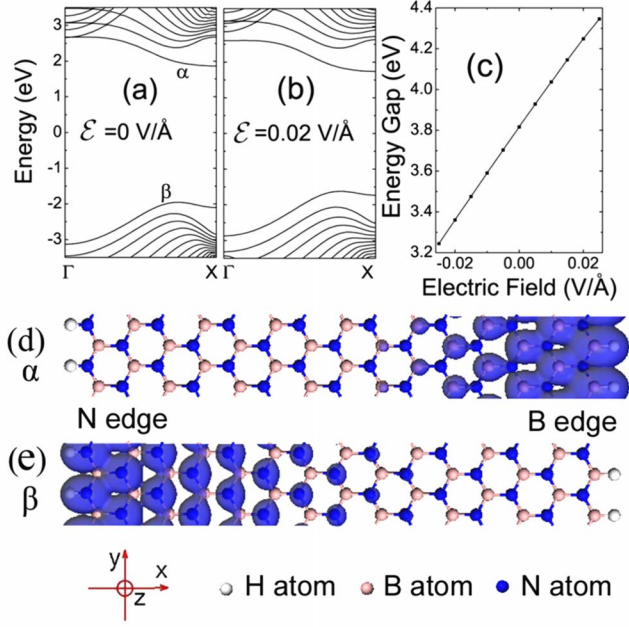


FIG. 1. (Color online) Electronic structure of 15-ZBNNR. (a) The energy bands without any electric field. The Fermi level is set to zero. (b) The energy bands with a transverse electric field  $\mathcal{E}$ , which is opposite to the  $x$  direction. (c) The band gap as a function of the transverse electric-field strength. (d) The partial charge density of the bottom of the lowest conduction band (band  $\alpha$ ). (e) The partial charge density of the top of the highest valence band (band  $\beta$ ). The isovalue is  $0.0067 e/\text{\AA}^3$ .

Pack scheme and 21  $k$  points were used in our calculations. The effect of electric field on an infinite system is generally a tough problem,<sup>28</sup> but the effect of a transverse electric field on nanoribbons/nanotubes is easy to deal with since the field is applied along the finite dimension of the system, which is modeled in our calculation by a sawtooth potential in a supercell geometry along the direction perpendicular to the nanoribbon/nanotube axis (for nanoribbons, the field is in the plane of the sheet). All geometries were optimized until the forces on the atoms were less than  $0.04$  eV/Å. A similar scheme is employed for BNNTs.

We start the discussion on BNNRs. In accordance with the previous convention,<sup>20,25</sup> here the BNNRs are labeled by the number of  $B-N$  chains along the ribbons, which defines the width of the ribbon. The ZBNNR with  $n$   $B-N$  chains is thus named as  $n$ -ZBNNR, while the ABNNR is named  $n$ -ABNNR. The outmost atoms of BNNRs are  $H$  passivated.

The calculated properties of the 15-ZBNNR, whose width is about  $33.18$  Å, are shown in Fig. 1. As found in previous calculations,<sup>29</sup> this material is a wide-gap semiconductor [see Fig. 1(a)] with a calculated Kohn-Sham band gap of  $3.82$  eV. The conduction-band bottom [band  $\alpha$  in Fig. 1(a)] consists of  $\pi$ -like orbitals localized at the  $B$  edge of ZBNNR with the major component on boron atoms as shown in Fig. 1(d), while the valence-band top [band  $\beta$  in Fig. 1(a)] localizes at the  $N$  edge with  $\pi$ -like orbitals on the nitrogen instead of boron atoms [Fig. 1(e)]. Accordingly, the conducting electrons and holes in this system are localized separately at the boron and nitrogen edges, which may give rise to interesting

transport and thermoelectric properties. The symmetry breaking of edges and the local residence of the valence band at the  $N$  edge give rise to a spontaneous transverse electric polarization, which will lead to a linear giant Stark effect (see below).

When a transverse electric field is applied to the system, the boron (nitrogen) atoms move along (against) the direction of the applied field slightly. This is consistent with the charge transfer from the boron atoms to the nitrogen atoms. The energy bands' structure of 15-ZBNNR with  $0.02$  V/Å electric field, which is opposite to the  $x$  direction, is plotted in Fig. 1(b). The energy of band  $\alpha$  decreases slightly while that of band  $\beta$  increases, consequently the energy gap narrows. The band gap is plotted as a function of the applied electric field in Fig. 1(c). A positive field broadens the gap while a negative field narrows the gap. This is a linear giant Stark effect. It is different from the effect in nanotubes<sup>1-7,11,12</sup> where the electric field is only able to reduce the energy gap. Within the field range we investigated in Fig. 1(c), the field dependence of the energy gap is well described by a linear law

$$E_g(\mathcal{E}) = E_{g,0} + eS_L\mathcal{E}, \quad (1)$$

where  $e$  is the electron charge,  $\mathcal{E}$  is the applied transverse electric-field strength, and  $S_L$  is a linear coefficient of the giant Stark effect, which is used to measure the ability of the electric field to modify the energy gap. For the 15-ZBNNR,  $S_L = 22.3$  Å. When the electric field is much larger, a nonlinear effect will appear and the energy gap may be even closed, which has been analyzed by Zhang and Guo<sup>8</sup> recently.

To further explore the role of symmetry in the giant Stark effect, we examined the ABNNR (20-ABNNR with a width of  $25.84$  Å) and presented the results in Fig. 2. As in the zigzag case, both the lowest conduction band (band  $\alpha$ ) and highest valence band (band  $\beta$ ) are  $\pi$ -like. However, the charge density of the two bands spreads across the ribbon plane [Figs. 2(d) and 2(e)] but not separate as in the zigzag case. As a result, the electric field has a different effect in ABNNRs [Fig. 2(c)]. The curve of the energy gap vs the transverse electric field  $\mathcal{E}$  is symmetric with respect to  $\mathcal{E} = 0$ , i.e., the positive field has the same effect as the negative one. The gap varies quadratically for small electric fields and has a zero slope at  $\mathcal{E} = 0$ , so it is a nonlinear giant Stark effect. For larger fields, the curve becomes linear and can be described by

$$E_g(\mathcal{E}) = E_{g,0} - eS_L|\mathcal{E}|, \quad (2)$$

with the coefficient  $S_L = 15.3$  Å. The perturbation of the field causes mixing among states within the conduction and valence subband complexes, and the resulting  $\alpha$  minimum and  $\beta$  maximum states move in opposite directions and locate locally at two edges, respectively [Figs. 2(f) and 2(g)]. These features are similar to what was observed in BNNTs.<sup>7</sup> The nonlinear effect under much stronger fields has been investigated recently,<sup>8</sup> which is beyond the interest of this work.

The giant Stark effect discussed above can be understood with a simplified physical model (Fig. 3). For ZBNNRs, the charge density of the conduction-band minimum state and

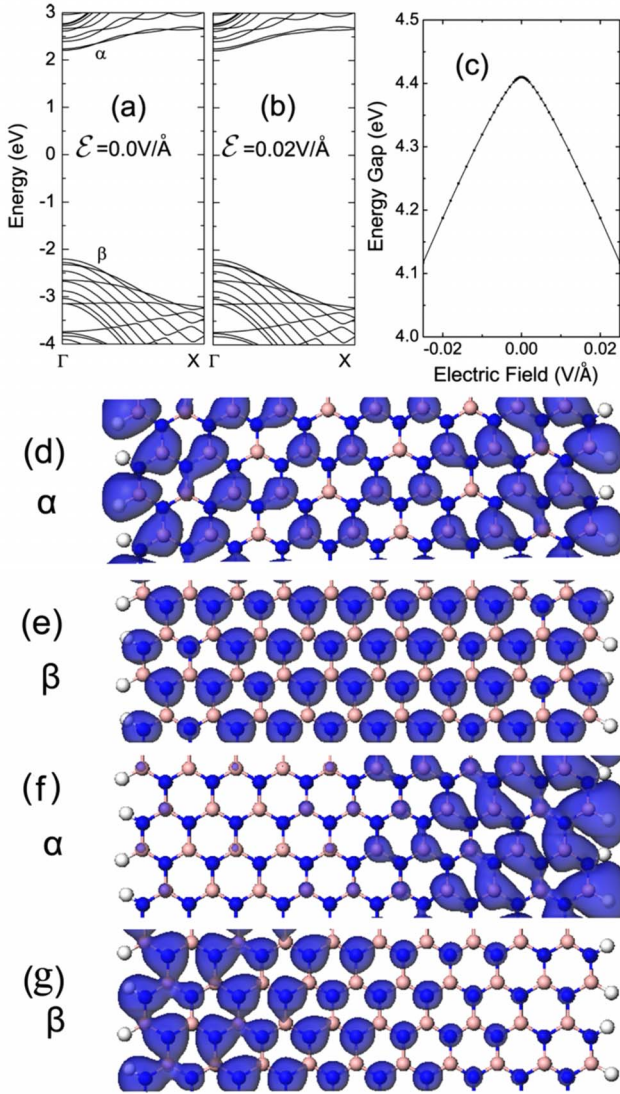


FIG. 2. (Color online) Electronic structure of 20-ABNNR. (a) The energy bands under zero electric field. (b) The energy bands with a transverse electric field of 0.02 eV/Å along the  $x$  direction. (c) The band gap as a function of the transverse electric field. (d), (e) The partial charge density of the bottom of the lowest conduction band (band  $\alpha$ ) and the top of the highest valence band (band  $\beta$ ) under zero electric field. (f), (g) The partial charge density of the bottom of band  $\alpha$  and the top of band  $\beta$  under the electric field of 0.02 eV/Å. The isovalue is 0.0067  $e/\text{Å}^3$ .

the valence-band maximum state is located at the ribbon edges [Figs. 1(d) and 1(e)]. Since the potential of the transverse electric field is  $e\mathcal{E}x$ , the change in the energy gap induced by the electric field can be approximated as

$$\Delta E_g = e\mathcal{E}\langle x \rangle_c - e\mathcal{E}\langle x \rangle_v, \quad (3)$$

where  $\langle x \rangle_c$  and  $\langle x \rangle_v$  are the centers of the conduction-band minimum state and the valence-band maximum state, respectively. So the energy gap linearly depends on the applied electric field and the giant Stark effect coefficient is given as (see Fig. 3)

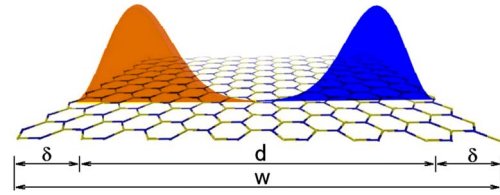


FIG. 3. (Color online) Schematic of the model to explain the giant Stark effect. The left (orange/light gray) wave and the right (blue/dark gray) wave represent the wave functions of the valence-band top and the conduction-band bottom, respectively. The ribbon width is  $w$  while the distance between the centers of the wave functions and the edges is  $\delta$ , so the distance between the centers of two wave functions is  $d = w - 2\delta$ .

$$S_L = \frac{1}{e} \frac{dE_g}{d\mathcal{E}} = \langle x \rangle_c - \langle x \rangle_v = d, \quad (4)$$

where  $d$  is the distance between the centers of the conduction-band minimum state and the valence-band maximum state. For ABNNRs, the electric field induces the mixing among subband states and the wave function of the resulting conduction-band minimum state moves along the direction of the electric field while that of the valence-band maximum moves against the field direction [Figs. 2(f) and 2(g)]. Both states get localized at the edges under strong fields and then the analysis in ZBNNRs is applicable here

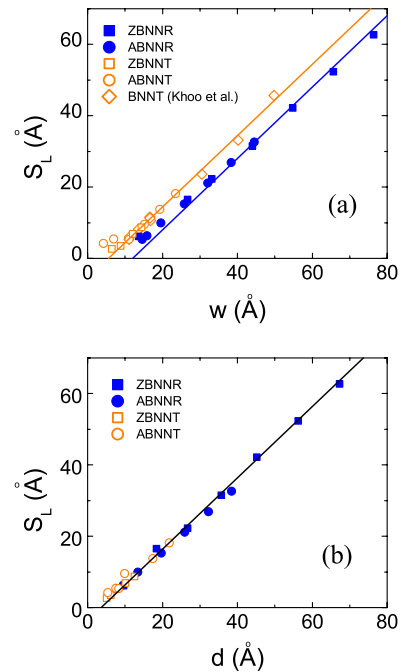


FIG. 4. (Color online) The linear coefficient of giant Stark effect ( $S_L$ ) as a function of (a) the ribbon width or tube diameter and (b) the distance between the centers of the conduction-band minimum and the valence-band maximum wave functions. Data points for BNNRs are represented by blue (dark gray) solid symbols while those for BNTs are represented by orange (light gray) open symbols. The data extracted from Khoo *et al.* (Ref. 7) are also inserted in (a) as open diamonds.

which also gives  $S_L=d$ . The obtained  $S_L$  values in Fig. 1 and Fig. 2 are smaller than the width of the ribbons, which is consistent with the picture of the model.

According to this model, there exists a scaling law for the giant Stark effect when the width is large enough. Denote  $\delta$  as the distance between the valence (conduction) wavefunction center and the ribbon edge and then we have  $d=w-2\delta$ , where  $w$  is the ribbon width (Fig. 3). Thus, the giant Stark effect coefficient is expressed as

$$S_L = w - 2\delta. \quad (5)$$

For large  $w$ , the valence-band maximum state at one edge is hardly affected by the opposite edge, and so is the conduction-band minimum. So  $\delta$  is a constant independent of  $w$  for large  $w$ . Consequently,  $S_L$  is expected to obey a linear scaling law on  $w$ , whose slope is predicted to be 1.0 and the intercept at  $w=0$  will give information about  $\delta$ . To test this scenario, we depicted the  $S_L$  data of various ZBNRs and ABNNRs in Fig. 4(a) as a function of  $w$  together with our calculated results of zigzag and armchair BN nanotubes and also data extracted from Fig. 3 of Khoo *et al.*<sup>7</sup> Although ZBNRs and ABNNRs have quite different responses to the transverse electric field, their  $S_L \sim w$  plots overlap into one group, which separates well from those of nanotubes. Two groups of data (nanoribbons and nanotubes) can be separately fitted using Eq. (5) with high accuracy [solid lines in Fig. 4(a)]. The fitted  $\delta$  value for nanoribbons, 6.0 Å, is larger than that for nanotubes, 2.8 Å, which can be explained from the fact that the induced conduction-band minimum and the valence-band maximum states extend along the tube wall which is perpendicular to the electric field (refer to Fig. 2 of Khoo *et al.*<sup>7</sup>) and thus the centers are closer to the edges than those in nanoribbons. To verify whether  $\delta$  is the

origin of the difference between the nanoribbon curve and the nanotube curve, we calculated the wave functions' center positions of the valence-band maximum and the conduction-band minimum and their distance  $d$ . The dependence of  $S_L$  on  $d$  for both nanoribbons and nanotubes is drawn in Fig. 4(b). It clearly demonstrates that the data of nanoribbons and those of nanotubes merge into a unified curve, which is well described by a straight line with a slope of 1.0 [solid line in Fig. 4(b)]. Compared to the  $S_L \sim w$  curves, the intercept of the  $S_L \sim d$  curve is closer to zero. Nevertheless, the intercept is not equal to zero, which slightly deviates from the prediction of the model [Eq. (4)]. A further detailed analysis indicates that the discrepancy is mainly contributed by the screening effect of the induced polarization under electric field (data not shown).

In summary, we have studied the giant Stark effect in BN nanoribbons and nanotubes using *ab initio* calculations. As affected by a transverse electric field, the ABNNRs and ZBNRs have quite different behaviors because of their different symmetries. A physical model was presented to understand the influence of electric field on the band gap, and the giant Stark coefficients of both BN nanoribbons and nanotubes were found to obey a universal scaling law where the coefficient depends linearly on the ribbon width or the tube diameters with a predicted slope of 1.0. The mechanism underlying the scaling law in these systems is general, so we expect the application of this mechanism to other semiconductors.

This work was supported by the Ministry of Science and Technology of China (Grants No. 2006CB605105 and No. 2006CB0L0601) and the National Natural Science Foundation of China (Grant No. 10674077).

\*Author to whom correspondence should be addressed; dwh@phys.tsinghua.edu.cn

<sup>1</sup>J. O'Keeffe, C. J. Wei, and K. J. Cho, *Appl. Phys. Lett.* **80**, 676 (2002).

<sup>2</sup>Y.-W. Son, J. Ihm, M. L. Cohen, S. G. Louie, and H. J. Choi, *Phys. Rev. Lett.* **95**, 216602 (2005).

<sup>3</sup>C.-W. Chen, M.-H. Lee, and S. J. Clark, *Nanotechnology* **15**, 1837 (2004).

<sup>4</sup>Y. H. Kim and K. J. Chang, *Phys. Rev. B* **64**, 153404 (2001).

<sup>5</sup>Y. Li, S. V. Rotkin, and U. Ravaioli, *Nano Lett.* **3**, 183 (2003).

<sup>6</sup>T. S. Li and M. F. Lin, *Phys. Rev. B* **73**, 075432 (2006).

<sup>7</sup>K. H. Khoo, M. S. C. Mazzoni, and S. G. Louie, *Phys. Rev. B* **69**, 201401(R) (2004).

<sup>8</sup>Z. H. Zhang and W. L. Guo, *Phys. Rev. B* **77**, 075403 (2008).

<sup>9</sup>V. Barone and J. E. Peralta, *Nano Lett.* **8**, 2210 (2008).

<sup>10</sup>C. H. Park and S. G. Louie, *Nano Lett.* **8**, 2200 (2008).

<sup>11</sup>T. Takenobu, Y. Murayama, and Y. Iwasa, *Appl. Phys. Lett.* **89**, 263510 (2006).

<sup>12</sup>M. Ishigami, J. D. Sau, S. Aloni, M. L. Cohen, and A. Zettl, *Phys. Rev. Lett.* **94**, 056804 (2005).

<sup>13</sup>Y. W. Son, M. L. Cohen, and S. G. Louie, *Nature (London)* **444**, 347 (2006).

<sup>14</sup>T. B. Martins, R. H. Miwa, A. J. R. da Silva, and A. Fazzio, *Phys. Rev. Lett.* **98**, 196803 (2007).

<sup>15</sup>A. Rycerz, J. Tworzydło, and C. W. J. Beenakker, *Nat. Phys.* **3**, 172 (2007).

<sup>16</sup>Z. Y. Li, H. Y. Qian, J. Wu, B. L. Gu, and W. H. Duan, *Phys. Rev. Lett.* **100**, 206802 (2008).

<sup>17</sup>R. Saito, M. Fujita, G. Dresselhaus, and M. S. Dresselhaus, *Appl. Phys. Lett.* **60**, 2204 (1992); J. W. Mintmire, B. I. Dunlap, and C. T. White, *Phys. Rev. Lett.* **68**, 631 (1992).

<sup>18</sup>A. Rochefort, D. R. Salahub, and P. Avouris, *J. Phys. Chem. B* **103**, 641 (1999); A. Rubio, D. Sanchez-Portal, E. Artacho, P. Ordejón, and J. M. Soler, *Phys. Rev. Lett.* **82**, 3520 (1999).

<sup>19</sup>J. Li, G. Zhou, L. Yang, J. Wu, and W. H. Duan, *Phys. Rev. B* **71**, 073409 (2005).

<sup>20</sup>K. Nakada, M. Fujita, G. Dresselhaus, and M. S. Dresselhaus, *Phys. Rev. B* **54**, 17954 (1996); K. Wakabayashi, M. Fujita, H. Ajiki, and M. Sigrist, *ibid.* **59**, 8271 (1999).

<sup>21</sup>Y. W. Son, M. L. Cohen, and S. G. Louie, *Phys. Rev. Lett.* **97**, 216803 (2006).

<sup>22</sup>A. Nagashima, N. Tejima, Y. Gamou, T. Kawai, and C. Oshima, *Phys. Rev. Lett.* **75**, 3918 (1995).

<sup>23</sup>M. Corso, T. Greber, and J. Osterwalder, *Surf. Sci.* **577**, L78

- (2005).
- <sup>24</sup>K. S. Novoselov, D. Jiang, F. Schedin, T. J. Booth, V. V. Khotkevich, S. V. Morozov, and A. K. Geim, Proc. Natl. Acad. Sci. U.S.A. **102**, 10451 (2005).
- <sup>25</sup>F. W. Zheng, G. Zhou, Z. R. Liu, J. Wu, W. H. Duan, B. L. Gu, and S. B. Zhang, arXiv:0804.4271 (unpublished).
- <sup>26</sup>N. Troullier and J. L. Martins, Phys. Rev. B **43**, 1993 (1991); L. Kleinman and D. M. Bylander, Phys. Rev. Lett. **48**, 1425 (1982).
- <sup>27</sup>D. Sanchez-Portal, O. E. Artacho, P. Ordejon, E. Artacho, and J. M. Soler, Int. J. Quantum Chem. **65**, 453 (1997).
- <sup>28</sup>Z. R. Liu, J. Wu, and W. H. Duan, Phys. Rev. B **69**, 085117 (2004).
- <sup>29</sup>J. Nakamura, T. Nitta, and A. Natori, Phys. Rev. B **72**, 205429 (2005).